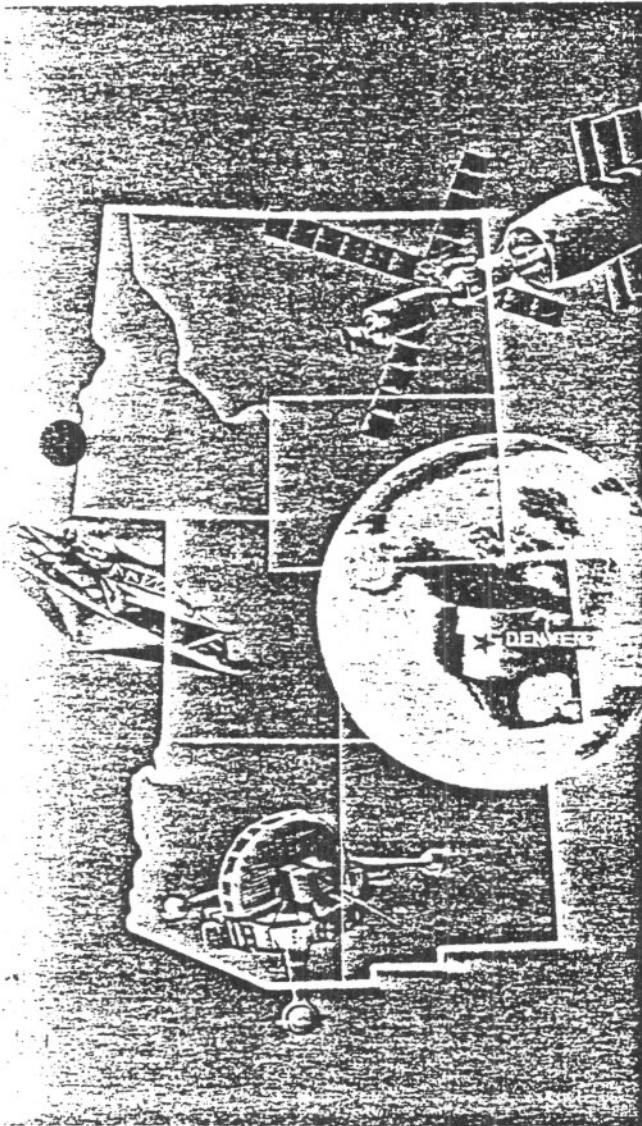# SPACE PROJECTIONS
from the
ROCKY MOUNTAIN REGION

THE MECHANICS & APPLICATIONS OF THE PLANETARY SWINGBY TECHNIQUE FOR OPTIMIZATION OF INTERPLANETARY TRAJECTORIES

Gary A. Flandro

University of Utah

AMERICAN *ASTRONAUTICAL* SOCIETY

Cosponsor:
AMERICAN INSTITUTE OF
AERONAUTICS AND ASTRONAUTICS

Rocky Mountain Sections

July 15—16, 1968   BROWN PALACE HOTEL, Denver, Colorado

THE MECHANICS AND APPLICATIONS OF THE PLANETARY

SWING-BY MANEUVER IN INTERPLANETARY MISSION DESIGN

G. A. Flandro*
University of Utah
Salt Lake City, Utah

INTRODUCTION

Modification of interplanetary trajectories by gravitational pertur-
bation of intermediate planets is not a new concept; Hohmann (1) studied
ballistic round trip trajectories to Mars and Venus almost fifty years ago.
More recently, investigators (2,3,4,5) have realized that a significant
change in vehicle heliocentric kinetic energy results from a midcourse
planetary encounter. Under favorable geometrical conditions this energy
can be utilized in reducing the launch energy and, consequently, the launch
vehicle size required to fly a given payload to the final target planet.
In some cases round-trip trajectories are also possible; the energy change
at the target planets being used to modify the trajectory for the return
leg. A very important application of the midcourse planetary encounter
maneuver is in reducing total trip time to the target. This has had an
especially profound effect on mission planning for unmanned exploration
of the outer solar system. For example, as compared to a direct ballis-
tic flight, travel time to the vicinity of Neptune can be reduced by a
factor of four by first passing the planet Jupiter (5). The latter planet,
which due to its large mass can produce a very large energy change, plays
an important role in several very interesting mission designs (4,5). Trip
time to all of the outer planets can be significantly reduced by use of
the Jupiter "swing-by" and an incredible "grand tour" mission passing Jupi-
ter, Saturn, Uranus, and Neptune is possible every 175 years; the next op-
portunity is in the 1976-1979 time period (5). The Jupiter encounter is
also capable of modifying the spacecraft trajectory into an out-of-the
ecliptic mission, a solar probe mission, or a galactic probe trajectory.
The latter missions would all require prohibitively large launch energy
if flown directly from the earth; the midcourse planetary encounter at
Jupiter reduces both required launch energy and the trip time in most
cases.

It is apparent that use of the midcourse planetary encounter (or
"swing-by" method as it will be referred to in what follows) to shape a
trajectory will play an increasingly important role in space mission de-
sign and it is essential that the mission analyst understand the mechanics
of the technique and the potential applications. Thus, it is the purpose

---

*Assistant Professor, Department of Mechanical Engineering

of this paper to: (1) clarify the theory of the planet swing-by maneuver and to indicate the mission design procedures which it requires and (2) to outline the basic applications. In the latter regard, a brief survey is given of swing-by missions which have already been studied in detail, and several new mission possibilities are suggested. In particular, the possibility of fast round-trip reconnaissance missions to the outer planets is evaluated. Also, optimum usage of a Jupiter swing-by in a solar system escape mission is explored, and the effect on galactic probe performance is evaluated.

MECHANICS OF THE MIDCOURSE PLANETARY ENCOUNTER ENERGY CHANGE

The mechanism by which the heliocentric energy of the space vehicle is changed by the gravitational perturbation during the passage of an intermediate planet is readily understood in terms of basic principles. To the spacecraft, the planet represents a force field moving relative to an inertial heliocentric coordinate system. The work done by this moving force changes the heliocentric kinetic energy as will now be demonstrated.

Let the heliocentric positions of the planet and the probe be designated by $\bar{\rho}$ and $\bar{R}$ respectively and the position of the probe relative to the planet by $\bar{r}$ as shown in Figure 1. Thus

$$\bar{R} = \bar{\rho} + \bar{r} \tag{1}$$

and the work done on the spacecraft by the planetary gravitational force is

$$W = \int_i^0 \bar{F}_p \cdot d\bar{R} = \int_i^0 \bar{F}_p \cdot (d\bar{\rho} + d\bar{r}) \tag{2}$$

Limits i and o refer to incoming and outgoing points on the sphere of influence. One may write the differential displacement vector in the form

$$d\bar{R} = \left(\frac{d\bar{\rho}}{dt}\right)dt + d\bar{r} \tag{3}$$

where $d\bar{\rho}/dt = \bar{v}_p = v_p\,\hat{P}$, is the velocity of the planet relative to the sun and P is a unit vector tangent to the planets' orbit in the direction of motion. The perturbing gravitational force is

$$\bar{F}_p = -\frac{\mu\,\bar{r}}{r^3} \tag{4}$$

where r is the planet-to-probe distance. The part of the work integral due to relative motion

$$\int_i^o \bar{F}_p \cdot d\bar{r}$$

is zero if it is assumed that there is no sensible influence on the planet's orbit due to passage of the probe. Introducing an angular position coordinate θ as shown in Figure 2, the work integral becomes

$$W = \int_{\theta_i}^{\theta_o} \bar{F}_p \cdot \bar{v}_p \left(\frac{d\theta}{dt}\right)^{-1} d\theta \quad\quad\quad (5)$$

where θ is measured in the plane of the encounter hyperbola from the axis as indicated in the figure. θ_i and θ_o refer to the angular position of points on the sphere of influence intersected by the incoming and outgoing hyperbolic asymptotes. Now the angular rate for a hyperbolic trajectory is

$$\frac{d\theta}{dt} = \frac{h}{r^2} = \frac{[\mu\, a(e-1)]^{\frac{1}{2}}}{r^2} \quad\quad\quad (6)$$

where

> h = angular momentum per unit mass of probe relative to the planet
> μ = gravitational constant of planet
> a = semi major axis of hyperbola
> e = eccentricity of hyperbola

From the Vis Viva integral, the relative speed at any point is

$$v = [\mu(2/r + 1/a)]^{\frac{1}{2}}$$

Thus, the incoming and outgoing relative speeds at the sphere of influence are

$$v_i = v_o = v_h = \sqrt{\frac{\mu}{a}}$$

where v_h is the hyperbolic excess speed. Thus, $a = \mu/v_h^2$ and the eccentricity may be written in terms of the deflection angle ψ as defined in Figure 2:

$$e = \sec\left(\frac{\pi-\psi}{2}\right) = \csc \psi/2$$

Thus

$$\frac{d\theta}{dt} = \frac{\mu \cot(\psi/2)}{v_h r^2} \quad\quad\quad (7)$$

ψ is given by

$$\psi = \cos^{-1}(\hat{I} \cdot \hat{O}) \tag{8}$$

where $\hat{I}$ and $\hat{O}$ are unit vectors pointing along the incoming and outgoing asymptotes as shown in Figure 2. Choosing a coordinate system aligned with the axis of the encounter hyperbola, one may write the unit vectors i and j defining a right-handed set in terms of I and O as follows:

$$\begin{cases} \hat{i} = \dfrac{\hat{I}-\hat{O}}{|\hat{I}-\hat{O}|} = \dfrac{\hat{I} - \hat{O}}{\sqrt{2(1 - \cos \psi)}} \\[4mm] \hat{j} = \dfrac{\hat{I}+\hat{O}}{|\hat{I}+\hat{O}|} = \dfrac{\hat{I} + \hat{O}}{\sqrt{2(1 + \cos \psi)}} \end{cases} \tag{9}$$

In this system, the probe position is

$$\bar{r} = (r \cos \theta)\hat{i} + (r \sin \theta)\hat{j}$$

Thus, the work integral becomes

$$W = \int_{-(\psi/2+\pi/2)}^{(\psi/2+\pi/2)} [- \frac{\mu}{r^2} v_p \frac{v_h r^2}{\mu} \tan \psi/2] \hat{P} \cdot [\frac{\cos \theta(\hat{I}-\hat{O})}{\sqrt{2(1 - \cos \psi)}} \tag{10}$$

$$+ \frac{\sin \theta(\hat{I}+\hat{O})}{\sqrt{2(1 + \cos \psi)}}]d\theta$$

Performing the integration

$$W = 2v_p v_h \hat{P} \cdot (\hat{O}-\hat{I}) \frac{\tan \psi/2 \sin(\psi/2 + \pi/2)}{\sqrt{2(1 - \cos \psi)}} \tag{11}$$

$$= v_p v_h \hat{P} \cdot (\hat{O}-\hat{I})$$

and if one neglects the change in $|\bar{r}|$ during the passage through the sphere of influence as compared to the change in $|\bar{\rho}|$ the increment of vehicle heliocentric total energy is equal to the work done by the moving gravitational perturbation. Thus

$$\Delta E = W = \nu_p \nu_h \, \hat{P} \cdot (\hat{O}-\hat{I}) \qquad\qquad (12)$$

which is the most useful form for swing-by performance calculations.

It is convenient to define a characteristic energy (c.f. Reference 5)

$$E^* \equiv 2 \, \nu_p \nu_h \qquad\qquad (13)$$

which represents the largest theoretically possible energy change; this corresponds to a point mass planet with vehicle passage at the center point and $\psi = 180°$. All of the geometrical aspects of the encounter are encompassed in an energy change index f such that the energy increment is

$$\Delta E = fE^* \qquad\qquad (14)$$

f is a number between -1 and 1 as given by

$$f \equiv \tfrac{1}{2} \, \hat{P} \cdot (\hat{O}-\hat{I}) \qquad\qquad (15)$$

For the point mass planet, $f = 1$ if the probe approaches in the $-\hat{P}$ direction (opposite to direction of heliocentric motion of the planet), and $f = -1$ if the probe approaches in the direction of the planet, passes infinitely close and executes a 180° deflection. Of course, $|f| < 1$ always due to the finite size of the planet so E^* can never be achieved in practice. The actual value of f depends on the direction of the approach asymptote and the total deflection angle ψ at the planet. The latter depends, of course, on the gravitational parameter μ, the distance of closest approach, and asymptotic approach speed:

$$\psi = 2 \sin^{-1} [1 + \frac{\nu_h^{\,2}}{\mu} (d + r_p)]^{-1} \qquad\qquad (16)$$

where r_p = radius of planet at point of closest approach and d = distance from planet surface (or atmospheric radius depending on definition of r_p). The maximum allowable deflection corresponds to a flight path grazing a forbidden sphere of radius $R_p = d + r_p$ where d is a minimum approach distance chosen to allow for guidance errors.

The geometrical interactions contained in (15) are readily interpreted graphically as illustrated in Figure 3. The vector $\hat{I}$ along the approach asymptote and $\hat{P}$ (unit vector in direction of planets' motion) are fixed by the orbital elements of the incoming trajectory and by the arrival date. A convenient reference angle between these two vectors is the approach angle ξ defined by

$$\xi = \cos^{-1}(-\hat{P} \cdot \hat{I}) \qquad (17)$$

For a given $\hat{I}$ and $\hat{P}$, the value of f and the departure asymptote are set by $\hat{O}$. The ougoing asymptote may lie anywhere in a cone with semi-vertex angle equal to the maximum deflection angle defined above (see Figure 3). It is useful to represent the direction of $\hat{O}$ in terms of the angle ζ between the planes formed by I and O and I and P as shown in the figure. Thus, in terms of these parameters, the energy change index is

$$f = \frac{1}{2} [\cos \xi (1 - \cos \psi) + \sin \xi (\sin \psi \cos \zeta)] \qquad (18)$$

where $\psi < \psi_{max}$ is set by the asymptotic speed and distance of closest approach as already indicated. For a given value of direction of approach (angle ξ), the optimum energy gain is attained by adjusting the point of closest passage to bring $\hat{O}$ as close to the direction of $\hat{P}$ as possible. This is accomplished by passing "behind" the planet as illustrated in Figure 4. Thus

$$f_{max \atop gain} = \begin{cases} \dfrac{\cos \xi + 1}{2} & \xi \geq (\pi - \psi_{max}) \\[4mm] \dfrac{\cos \xi - \cos (\psi_{max} + \xi)}{2} & \xi < (\pi - \psi_{max}) \end{cases} \qquad (19)$$

Maximum decrease in heliocentric energy is accomplished by passing in front of the planet as shown in Figure 4. The corresponding values of f are

$$f_{max \atop loss} = \begin{cases} \dfrac{\cos \xi - 1}{2} & \xi \leq \psi_{max} \\[4mm] \dfrac{\cos \xi - \cos (\psi_{max} - \xi)}{2} & \xi > \psi_{max} \end{cases} \qquad (20)$$

Equations (19) and (20) are useful in checking actual values of f in conic trajectory runs against attainable values. In such computations, ξ and ζ are fixed by constraints imposed by launch date and launch energy. Trajectory optimization is accomplished by varying these quantities and blanketing the launch opportunity of interest with a sufficiently fine grid of trajectories that optimum points may be determined graphically (c.f. References 4, 5, 6, 7). It is also of interest to determine what energy change could be accomplished in a given situation if control of all parameters were possible. This control might be available for example by use of low-thrust propulsion on the pre-midcourse encounter trajectory to optimize the encounter geometry. For a given ν_h, there is a maximum value for the deflection angle ψ, and this deflection must be used to optimize

ΔE. Thus, assuming ξ can be controlled, f(and thus ΔE) is maximum if $\hat{P}$ is made coincident with the axis of the vector O-I (see Figures 2 and 3); f is minimum if $\hat{P}$ is opposite to $(\hat{O}-\hat{I})$ and $\cos^{-1}(\hat{O}\cdot\hat{I}) = \psi_{max}$. Note that the maximum and minimum values differ only in sign. Thus, for a given hyperbolic approach speed, the optimum energy change results if approach angle equals the optimum value

$$\xi_{opt} = \frac{\pi}{2} \mp \frac{\psi_{max}}{2} \qquad (21)$$

where the upper sign corresponds to energy gain; lower sign corresponds to energy loss. Values of energy change index corresponding to the optimum approach geometry are

$$f_{opt} = \pm \sin\left(\frac{\psi_{max}}{2}\right) \qquad (22)$$

where the same sign convention obtains. Finally, for a given ν_h, the optimum energy change is

$$\Delta E_{opt} = \pm (2\nu_p\nu_h)f_{opt} \qquad (23)$$

This relation is plotted vs ν_h in Figure 5 for all planets of the solar system. Note that ΔE_{opt} increases with ν_h only up to a certain critical hyperbolic approach speed after which there is a performance decline. This is because ψ_{max} decreases rapidly with ν_h after the critical point is reached, negating the linear increase in E* with ν_h. The E* curve for Jupiter is shown on Figure 5 for comparison.

Assuming that not only approach angle, but also hyperbolic speed may be controlled, it is of interest to determine analytically the optimum approach speed and corresponding global optimum energy change. Manipulating Equation (23)

$$\Delta E_{opt} = 2\nu_p\nu_h \sin\left(\frac{\psi_{max}}{2}\right)$$

but

$$\frac{\psi_{max}}{2} = \sin^{-1}\left(\frac{\mu}{\mu + \nu_h^2 R_p}\right)$$

where $R_p = d + r_p$ is the minimum allowable passage distance from the center of the planet. Thus, for any ν_h,

$$\Delta E_{opt} = \frac{2\nu_p \nu_h}{1 + \frac{\nu_h^2 R_p}{\mu}} \qquad (24)$$

which clearly shows the dependence on ν_h. For a given planet (ν_p and μ fixed), this expression has a stationary point at

$$(\nu_h)_{CRIT} = \sqrt{\frac{\mu}{R_p}} \qquad (25)$$

Thus, the global optimum energy change results when ν_h is equal to a critical value which depends only on the physical characteristics of the encounter planet. It is interesting to note that this critical speed is just the circular satellite velocity of the planet at an altitude equal to the minimum allowable approach distance. We may now summarize the conditions for global optimum energy change:

$$\begin{cases} f_{\substack{GLOBAL \\ OPTIMUM}} = \pm \sin\left(\frac{\psi_{max}}{2}\right)_{\nu_h = (\nu_h)_{opt}} = \pm 1/2 \qquad (26) \\ \\ \Delta E_{\substack{GLOBAL \\ OPTIMUM}} = \pm \nu_p \sqrt{\frac{\mu}{R_p}} \end{cases}$$

The approach angle required to achieve this energy change is thus

$$\xi_{\substack{GLOBAL \\ OPTIMUM}} = \frac{\pi}{2} \mp \sin^{-1}(1/2) = \begin{cases} 60^o \text{ energy gain} \\ 120^o \text{ energy loss} \end{cases} \qquad (27)$$

The values of $(\nu_h)_{opt}$ and $\Delta E_{\substack{GLOBAL \\ OPTIMUM}}$ are given in Table 1 for all planets of the solar system except Pluto whose physical parameter are not well known. $\Delta E_{\substack{GLOBAL \\ OPTIMUM}}$ for Jupiter exceeds that for any other planet by at least a factor of two. It is interesting that Venus, not Saturn (the second most massive planet) is second best resulting mainly from the high ν_p value due to its proximity to the sun. Jupiter's immense potential ΔE results, of course, from its large mass and relatively high density. It is of interest to note that $\Delta E_{\substack{GLOBAL \\ OPTIMUM}}$ for Jupiter is about five times larger than the kinetic energy imparted to the spacecraft by the launch vehicle to achieve an Earth-Jupiter trajectory. Thus, a truly incredible energy boost is available in a Jupiter swing-by maneuver. In what follows, some of the potential application of this energy boost are discussed.

APPLICATIONS OF THE SWING-BY MANEUVER

In this section the applications of the above theory are discussed.
Several important mission concepts which have been studied extensively
are first briefly summarized. Two new potential applications using Jupi-
ter swing-by energy are then presented: (1) Optimum usage of Jupiter en-
counter in a galactic probe mission and (2) Possibility of round-trip per-
formance in Jupiter swing-by missions to the outer planets.

Applications of the planetary swing-by method are conveniently cate-
gorized as follows: (1) Use of encounter energy to decrease required trip
time and/or required launch energy, (2) Use of encounter energy to shape
flight path as in a round-trip mission. The second mission type was the
first to be studied extensively (1,2,3,4,8,9) and the reader is referred
to the many published accounts for detailed discussions of trajectory
characteristics. The most interesting round-trip mission applications in-
volve manned reconnaissance of Venus and Mars.

The next decade abounds in useful mission possibilities of the first
type. Of considerable potential are the Earth-Venus-Mercury opportunities
(4,7,8,9,10). These trajectories utilize the loss of heliocentric energy
resulting from passage behind Venus to reduce the launch energy at Earth
required to reach Mercury. A similar application of the potent Venus
swing-by energy is useful in solar probe missions (11). Jupiter domi-
nates the field in potential applications as already indicated. Of con-
siderable interest (5,12,13) are missions to the outer solar system us-
ing heliocentric energy gained in Jovian encounters. In these trajec-
tories, the primary use of the Jovian energy boost is in reduction of
required time of flight. Table 2 shows the effect on trip time to each
of the outer planets and the optimum launch dates for such missions.
In each case the swing-by results are compared to minimum energy balli-
stic results, and the trajectory figures are based on the minimum bal-
listic launch energy to the target planet. A rare mission opportunity
(available every 175 years) is the "grand tour" which allows passage
of each of the outer planets (Jupiter, Saturn, Uranus, and Neptune) in
a single flight (5). Payload on any of the missions just discussed can
be enhanced through the use of optimized low-thrust electric propulsion.
The combination of solar-electric propulsion with the Jupiter swing-by
method was discussed by Flandro (6), and it was shown that payload is
typically tripled as compared to the purely ballistic swing-by trajec-
tories. Figure 6 shows the flight path for an optimized solar electric
Earth-Jupiter-Saturn mission. The trajectory first loops in toward the
sun, as is typical of solar electric vehicles, to optimize usage of
available solar energy flux. Minovitch (10) has suggested use of Jupi-
ter swing-by in solar probe, out-of-the-ecliptic and deep-space missions.

In studying the list of proposed swing-by missions, one notices
that the most useful trajectories all involve either Jupiter or Venus
encounters, and that these are the planets most able to impart a sig-
nificant encounter energy change. Useful swing-by maneuvers at other
planets are quite rare due to the limited energy gain available. For

example Martian encounters are applied mainly in round-trip missions, and in many such trajectories the swingby energy must be supplemented by a propulsion maneuver. Minovitch has examined use of gravitational perturbations of the Earth itself (14), and in particular assessed the possibility suggested earlier by Roy (15) of an out-of-the-ecliptic trajectory utilizing energy gained when the space vehicle re-encounters the Earth. The initial results indicated that no significant performance gains could be achieved in this manner.

Formidable energy is required for galactic probe missions to extra-solar space, and it is of interest to assess the potential application of the Jupiter encounter maneuver in such missions. Minovitch (10) pointed out that any Earth-Jupiter trajectory can be made hyperbolic relative to the sun by a close Jovian encounter. The optimum usage of the potential energy gain has not been previously discussed. The conditions for an optimum encounter were established in a foregoing section of the present paper and these can be used to assess the maximum usage of the Jovian gravitational energy boost. It is assumed that the Earth-Jupiter leg of the trajectory can be controlled such that optimum hyperbolic encounter velocity and approach angle are obtained. It is clear that such control can be achieved through use of electric propulsion devices, but no attempt is made here to establish the corresponding Earth-Jupiter flight path on vehicle performance and payload figures; we wish only to establish the maximum possible effect on galactic probe performance. Using Equations (26) and (27) one finds that the optimum hyperbolic approach velocity at Jupiter is $(\nu_h)_{opt} = 42.5$ km/sec and that if Jupiter is approached at this speed in the ecliptic plane with $\xi = 60°$, the global optimum energy increase of

$$\Delta E_{\substack{GLOBAL \\ OPTIMUM}} = 555 (km/sec)^2$$

is achieved. Heliocentric velocity vector of the spacecraft in polar coordinates before encounter is $\bar{\nu}_i = (36.9) e_r - (8.2) \hat{e}_\phi$ (km/sec) where $\hat{e}_\phi$ is nearly coincident with unit vector $\hat{P}$ in the direction of Jupiter's heliocentric motion; post-encounter velocity is $\bar{\nu}_0 = (36.9)\hat{e}_r + (34.3)\hat{e}_\phi$ (km/sec). Notice that only the tangential velocity is altered in an optimum encounter, and that the trajectory deflection angle is 60° relative to the planet and 55.5° relative to the sun. Thus, the vehicle must achieve a significant (already hyperbolic) radial speed before encounter. The heliocentric speeds before and after encounter are 37.8 km/sec and 50.4 km/sec respectively. The increase in vehicle speed due to Jupiter swing-by is 12.6 km/sec; a percentage velocity increase of exactly 33.3 per cent. The resulting hyperbolic orbit has eccentricity $e = 9.34$ and hyperbolic excess speed relative to the sum of $\nu_\infty = 46.9$ km/sec. Since the Jupiter encounter and solar escape phases of such a high-energy trajectory take place in a relatively short time, one may readily estimate performance by assuming constant interstellar cruise speed equal to ν_∞. For example, a ten-year flight would take the probe $1.48 \cdot 10^{10}$ km or about 100 astronomical units into interstellar space.

This assumes unpowered flight after Jupiter encounter, and it is useful to compare this performance with that of a similar vehicle without the Jovian energy boost. Thus, without close passage of Jupiter the same vehicle would achieve a hyperbolic excess speed of only 32.9 km/sec and would require over 14 years to reach the same distance from the sun.

The interest in missions to the outer planets via the Jupiter encounter has prompted investigation into the possible refinements. It would be quite useful to bring the payload from such a mission closer to the Earth for date retrieval after the final target planet is reached. This is possible if geometrical conditions at the target required for the necessary modification of the trajectory do not degrade the data collection process. One must also investigate the representative approach geometry and hyperbolic speeds to determine the availability of the necessary energy increment. Table 3 summarizes this data for a typical set of Jupiter swing-by trajectories to Saturn, Uranus, and Neptune. Both low and moderately high launch energy trajectories are represented. Notice that a round-trip trajectory or one with perihelion distance less than the orbital radius of the target planet requires that the available maximum encounter deflection angle ψ_{max} be greater in magnitude than the approach angle ξ. If ψ_{max} is less than ξ, the post-encounter orbit is either hyperbolic or elliptical (with probe moving toward aphelion after encounter). If ψ_{max} is greater than ξ, the radial post-encounter heliocentric velocity is negative and it is possible to enter an elliptical return orbit (with probe moving toward perihelion). Since ψ_{max} decreases rapidly with approach speed ν_h, round-trip Jupiter swing-by trajectories to the outer planets are only possible for the lower launch energies as indicated in Table 3. This, of course, results from the strong dependence of ν_h at the target on launch energy. Thus, the penalty for return of the probe toward the Earth's orbit is the increased flight time characteristic of the lower energy trajectories. For example, for the Earth-Jupiter-Saturn trajectories of Table 3, time-of-flight to Saturn is 3.6 years for the lower launch energy with the possibility for direct return to the inner solar system; for the high launch energy trajectory, the flight time is reduced to 2.3 years, but the perihelion of the post-encounter orbit is 4 A.U. The mission designer must perform a tradeoff between the outgoing and incoming trajectory characteristics to optimize the overall mission profile. Obviously one must also give due attention to the many other design constraints such as Saturn ring system constraints, occulation zones, instrumentation and communications look-angles, and so on. It is significant, however, that the designer has the option to return the vehicle to the vicinity of the Earth after the final planetary encounter.

CONCLUDING REMARKS

It is evident that application of the midcourse planet encounter maneuver or swing-by technique will play an important role in space exploration. The improvements in payload and reduced trip time are truly significant as well as the greatly increased design flexibility afforded the mission analyst. Combination of this method with other

advanced mission techniques such as use of low thrust electric propulsion will make planetary exploration truly practical. It has been shown (6) that the combination of low thrust solar electric propulsion with Jupiter or Venus swing-by will allow unmanned exploration of the entire solar system utilizing launch vehicles of very modest size. The ultimate feasibility of advanced missions of the type suggested will depend largely on improvements in guidance accuracy, system reliability, and Earth-based communications and tracking networks.

REFERENCES

1. Hohmann, W., <u>Die Erreichbarkeit der Himmelskoerper</u>. Munich: Oldenburg Publishing Corporation. 1925.

2. Crocco, G. A., "One-Year Exploration Trip, Earth-Mars-Venus-Earth." <u>Proceedings of the VIII International Astronautical Conference, Rome</u>. 1956.

3. Ehricke, K. A., <u>Space Flight. II: Dynamics</u>. New York: D. Van Nostrand Company. 1962.

4. Minovitch, M. A., "Determination and Characteristics of Ballistic Interplanetary Trajectories under the Influence of Multiple Planetary Attractions." <u>Technical Report No. 32-464</u>, Jet Propulsion Laboratory. 1963.

5. Flandro, G. A., "Fast Reconnaissance Missions to the Outer Solar System Utilizing Energy Derived from the Gravitational Field of Jupiter." <u>Astronautica Acta</u>. <u>12</u>:4. 1966.

6. Flandro, G. A., "Solar Electric Low-Thrust Missions to Jupiter with Swing-by Continuation to the Outer Planets." <u>Journal of Spacecraft and Rockets</u> (in press).

7. Sturms, F. M., "Trajectory Analysis of an Earth-Venus-Mercury Mission in 1973." <u>Technical Report No. 32-1062</u>, Jet Propulsion Laboratory. 1967.

8. Ross, S., "Trajectory Design for Planetary Mission Analysis." <u>AAS Preprint No. 65-130</u>. December 1965.

9. Sohn, R. L., et al, "Trajectories for Unmanned Interplanetary Missions." <u>AAS Preprint No. 65-30</u>. February 1965.

10. Minovitch, M. A., "Utilizing Large Planetary Perturbations for the Design of Deep Space, Solar Probe, and Out-of-Ecliptic Trajectories." <u>Technical Report No. 32-849</u>, Jet Propulsion Laboratory. 1965.

11. Casal, F. G. and Ross, S., "The Use of Close Venusian Passages During Solar Probe Missions." <u>AAS Preprint No. 65-31</u>. 1965.

12. Niehoff, J. C., "An Analysis of Gravity Assisted Trajectories to Solar System Targets." <u>AIAA Paper No. 66-10</u>. 1966.

13. Deerwester, J. M., "Jupiter Swing-by Missions to the Outer Planets." <u>AIAA Paper No. 66-536</u>. 1966.

14. Minovitch, M. A., "Evaluation of Prposed Free-Fall Earth-Earth-Out of Ecliptic Trajectories." Technical Memorandum 312-739, Jet Propulsion Laboratory. 1966.

15. Roy, A. E., "On the Use of Interplanetary Probe Orbits of Periods Commensurable with One Year." Astronautics Acta. 9, 31. 1963.

TABLE 1

OPTIMUM ENCOUNTER APPROACH SPEEDS

AND ENERGY INCREMENTS

PLANET	$(\nu_h)_{opt}$ (km/sec)	$\Delta E_{global\ opt}$ (km/sec)^2
Mercury	2.94	140
Venus	7.23	254
Earth	7.91	236
Mars	3.60	87
Jupiter	42.52	555
Saturn	25.63	246
Uranus	15.05	102
Neptune	16.59	90

TABLE 2

COMPARISON OF DIRECT AND SWING-BY TRAJECTORIES

TO THE OUTER PLANETS

Target Planet	Minimum Launch Energy (km^2/sec^2)	Optimum Launch Date with Jupiter Swing-by	Minimum Energy Trip Time Without Swing-by (years)	Trip Time with Jupiter Swing-by and Minimum Ballistic Launch Energy (years)
Saturn	109	5 October 1978	6.1	3.0
Uranus	126	9 October 1978	16.0	5.5
Neptune	135	11 November 1979	30.7	7.4
Pluto	135	8 September 1977	45.7	7.7

TABLE 3

EFFECT OF LAUNCH ENERGY ON POST-ENCOUNTER TRAJECTORIES

WITH MAXIMUM HELIOCENTRIC ENERGY LOSS

Mission	Launch Date	Launch Energy (km/sec)	Hyperbolic Excess Speed at Terminal Planet (km/sec)	Approach Angle at Terminal Planet ξ (deg)	Max. Deflection Angle ψ_{max} (deg)	Post-Encounter Radial Velocity (km/sec)	Post-Encounter Tangential Velocity (km/sec)	Eccentricity of Post-encounter orbit ε	Perihelion of post encounter orbit A.U.
Earth-Jupiter-Saturn	3 October 1978	100	9.72	83.2	122	- 6.09	2.07	.97	.22
	11 October 1978	150	19.53	100.0	76	7.93	- 8.26	.76	4.02
Earth-Jupiter-Uranus	19 October 1978	100	6.11	69.8	120	- 4.69	2.87	.87	1.85
	11 October 1978	130	19.99	91.7	46	14.31	- 7.17	2.24	6.72
Earth-Jupiter-Neptune	22 November 1980	110	7.67	69.2	117	- 5.69	0.26	.99	.03
	26 November 1980	150	19.82	86.6	52	11.25	-10.89	5.16	19.7

FIG. I — GEOMETRY

FIG. 2 – ENCOUNTER HYPERBOLA

FIG. 3 - GEOMETRY OF ENERGY OF ENERGY CHANGE INDEX

ψ_{max}

ΔE

V_P

ENERGY LOSS

ψ_{max}

ΔE

V_P

ENERGY GAIN
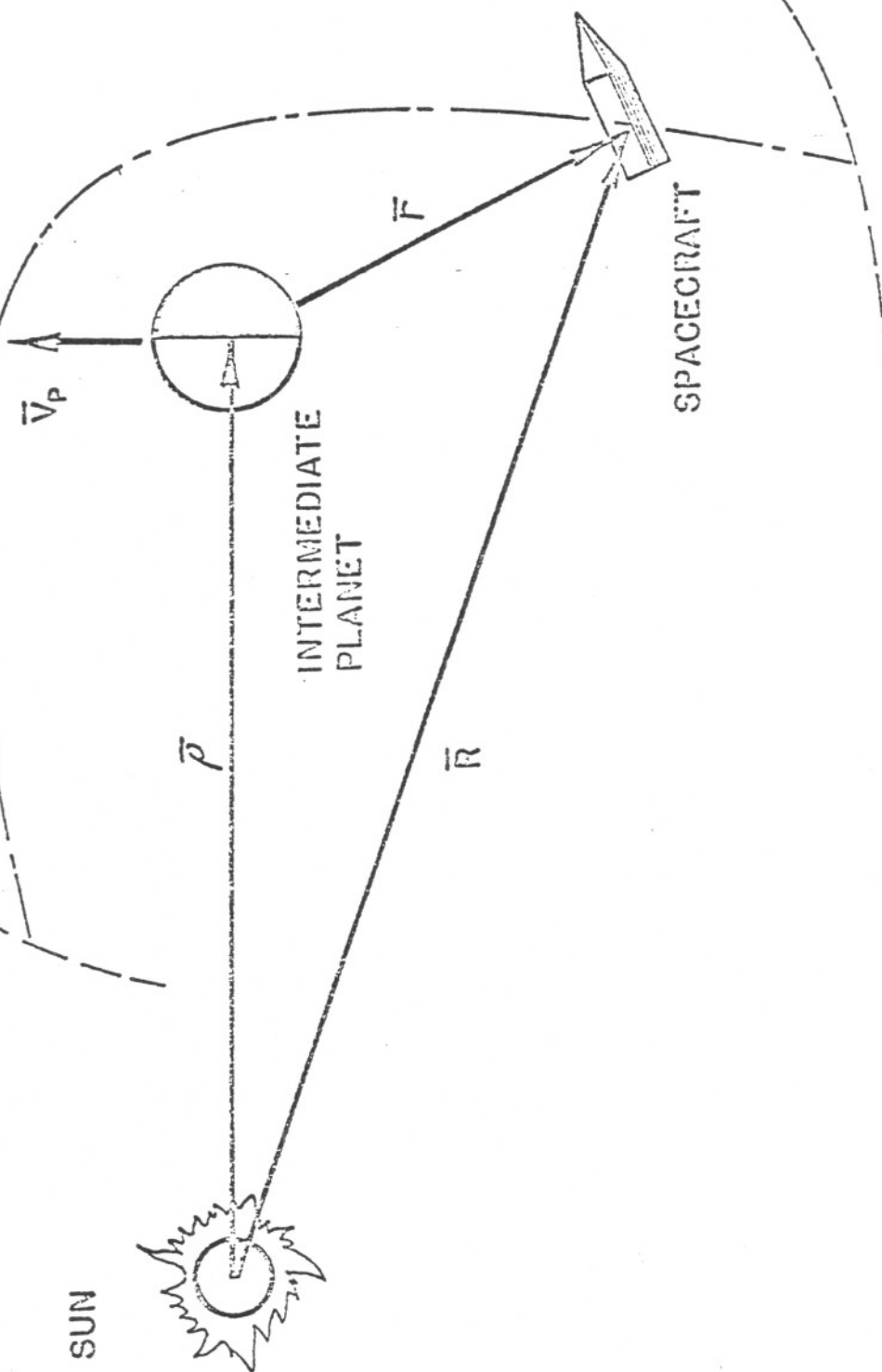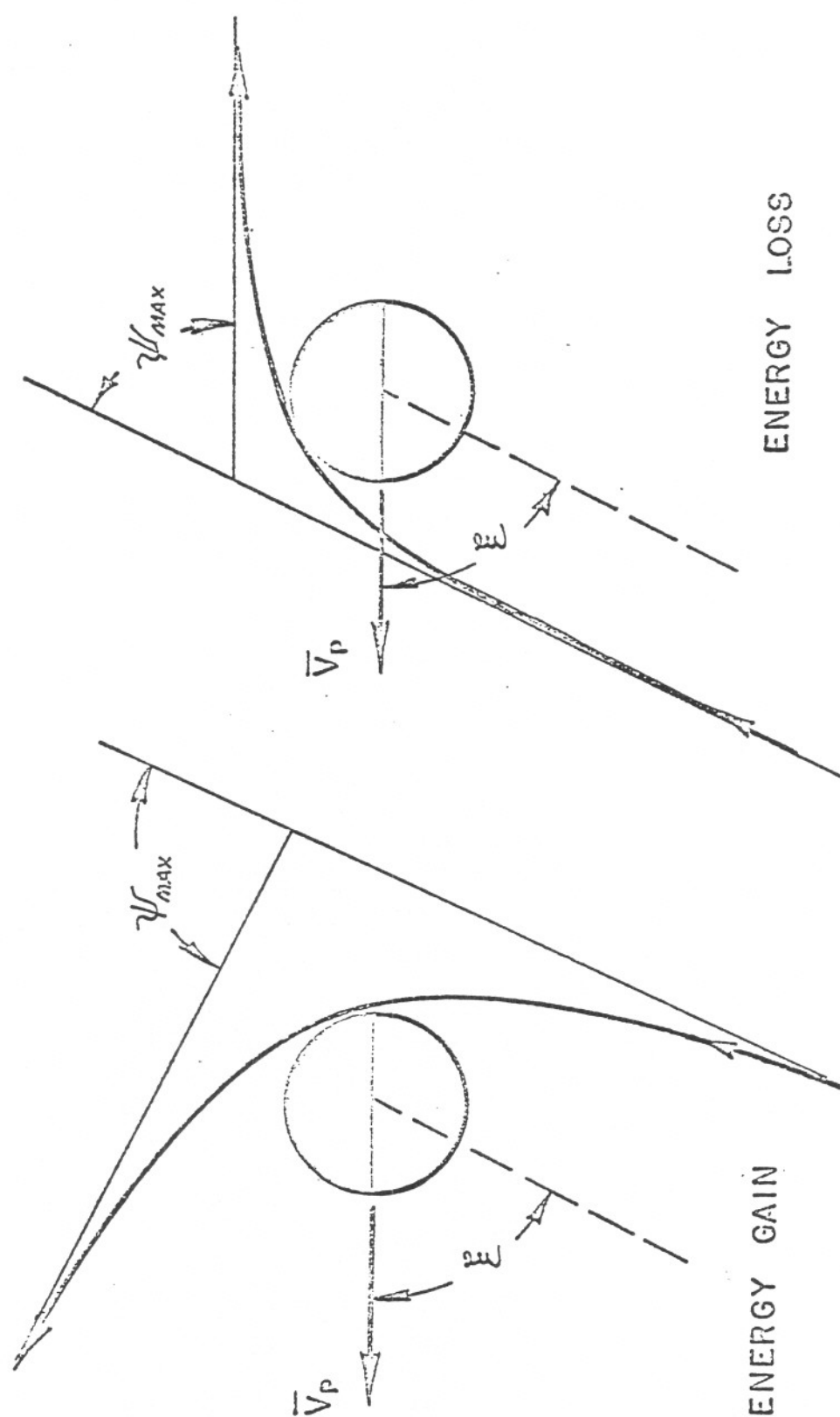
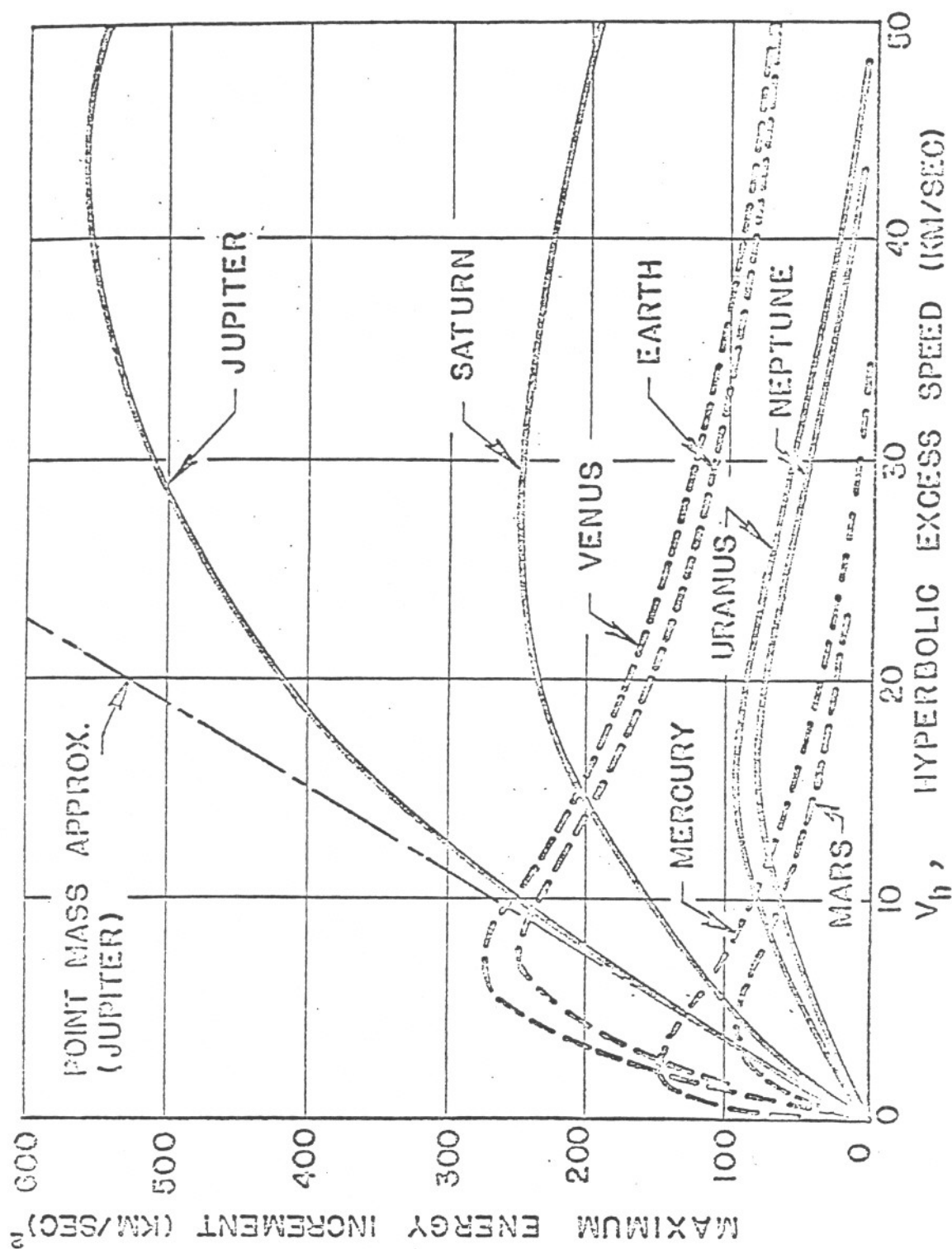FIG. 4 - OPTIMUM ENERGY CHANGE FOR GIVEN APPROACH ANGLE
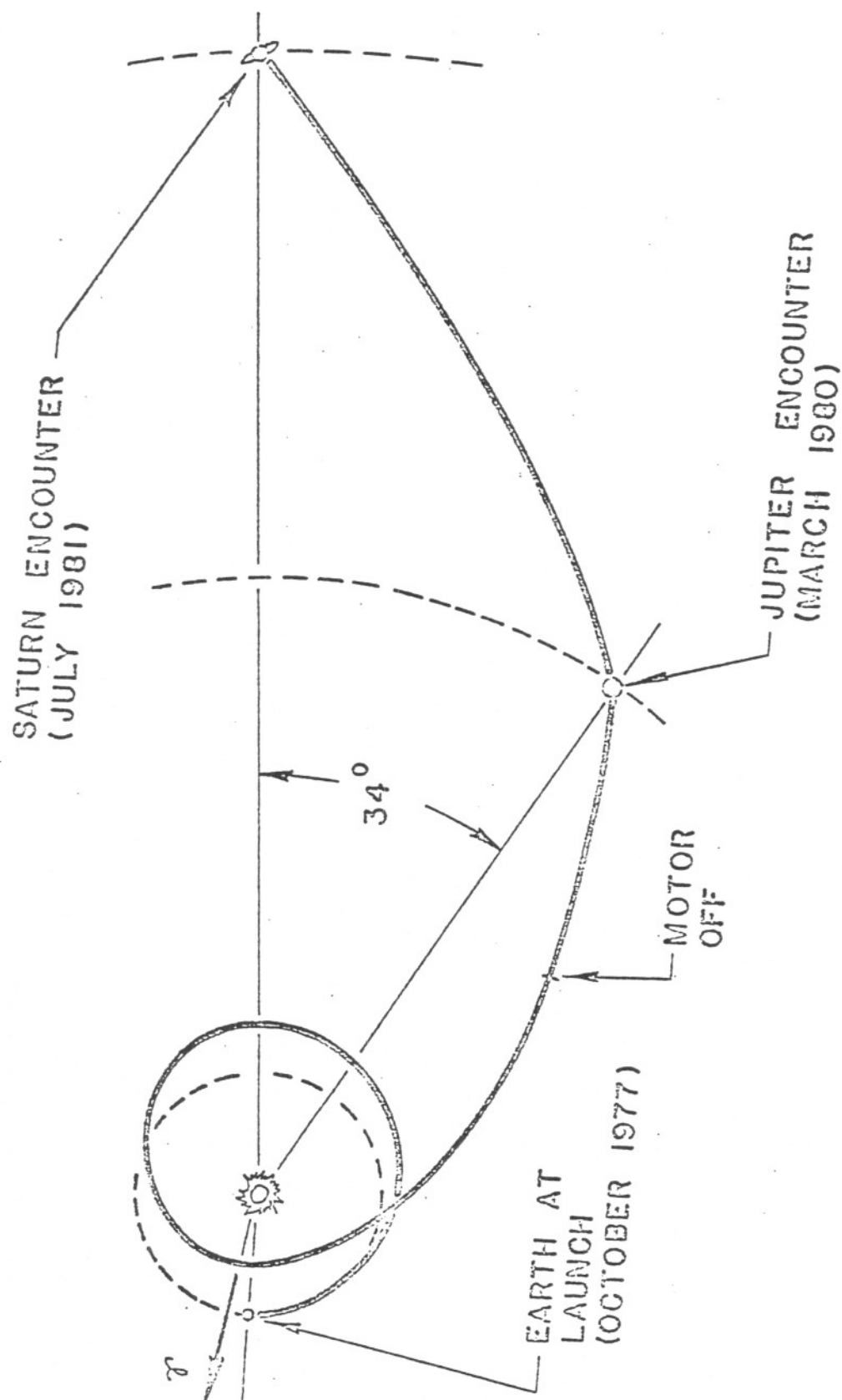
FIG. 5 – MAXIMUM ENERGY INCREMENT VS. V_h

FIG. 6 - JUPITER SWING-BY MISSION TO SATURN WITH SOLAR ELECTRIC LOW-THRUST PROPULSION

SATURN ENCOUNTER (JULY 1981)

JUPITER ENCOUNTER (MARCH 1980)

34°

MOTOR OFF

EARTH AT LAUNCH (OCTOBER 1977)